



Sialic acids attached to N- and O-glycans within the Na_v1.4 D1S5–S6 linker contribute to channel gating



Andrew R. Ednie, Jean M. Harper, Eric S. Bennett *

Department of Molecular Pharmacology and Physiology, University of South Florida Morsani College of Medicine, Tampa, FL 33612, USA

ARTICLE INFO

Article history:

Received 29 July 2014

Received in revised form 9 October 2014

Accepted 23 October 2014

Available online 30 October 2014

Keywords:

Voltage-gated Na⁺ channels

Ion channel gating

Sialic acids

Neuraminic acid

N-glycosylation

O-glycosylation

ABSTRACT

Background: Voltage-gated Na⁺ channels (Na_v) are responsible for the initiation and conduction of neuronal and muscle action potentials. Na_v gating can be altered by sialic acids attached to channel N-glycans, typically through isoform-specific electrostatic mechanisms.

Methods: Using two sets of Chinese Hamster Ovary cell lines with varying abilities to glycosylate glycoproteins, we show for the first time that sialic acids attached to O-glycans and N-glycans within the Na_v1.4 D1S5–S6 linker modulate Na_v gating.

Results: All measured steady-state and kinetic parameters were shifted to more depolarized potentials under conditions of essentially no sialylation. When sialylation of only N-glycans or of only O-glycans was prevented, the observed voltage-dependent parameter values were intermediate between those observed under full versus no sialylation. Immunoblot gel shift analyses support the biophysical data.

Conclusions: The data indicate that sialic acids attached to both N- and O-glycans residing within the Na_v1.4 D1S5–S6 linker modulate channel gating through electrostatic mechanisms, with the relative contribution of sialic acids attached to N- versus O-glycans on channel gating being similar.

General significance: Protein N- and O-glycosylation can modulate ion channel gating simultaneously. These data also suggest that environmental, metabolic, and/or congenital changes in glycosylation that impact sugar substrate levels, could lead, potentially, to changes in Na_v sialylation and gating that would modulate AP waveforms and conduction.

© 2014 Elsevier B.V. All rights reserved.

1. Introduction

The regulated gating and expression of voltage-gated ion channels (VGICs) are vital to cardiac, neuronal, and skeletal muscle electrical signaling primarily through the generation of action potentials (AP). Voltage-gated Na⁺ channels (Na_v) are responsible for the initiation and conduction of the AP. AP waveforms and conduction can be modulated through physiological and (remodeled through) pathological changes in ion channel expression and/or function [1–3].

Abbreviations: VGICs, voltage-gated ion channels; AP, action potentials; Na_v, voltage-gated Na⁺ channels; CHO, Chinese Hamster Ovary; K_v, voltage-gated K⁺ channel; hSkM1, human adult skeletal muscle voltage-gated Na_v channel, Na_v1.4; Na_v1.4/1.5D1S5–6, Na_v1.4 chimera in which the D1S5–S6 loop of hNa_v1.5 replaced the hNa_v1.4 loop; Gal, Galactose; GalNAc, N-acetylgalactosamine; GlcNAc, N-acetylglucosamine; MW, apparent molecular weight; G–V, Conductance–voltage; V_{1/2}, voltage of half-activation; V_h, voltage of half-inactivation; K_a, Boltzmann slope factor for activation; K_i, inactivation; SSI, Steady-state inactivation; τ_h, inactivation time constants; τ_{rec}, time constant for recovery from fast inactivation; SSA, steady-state activation; hERG, human ether-a-go-go

* Corresponding author at: Department of Molecular Pharmacology & Physiology, Morsani College of Medicine, University of South Florida, MDC 8, 12901 Bruce B. Downs Blvd Tampa, FL 33612–4799, USA. Tel.: +1 813 974 1545; fax: +1 813 974 3079.

E-mail address: esbennet@health.usf.edu (E.S. Bennett).

VGICs are heavily glycosylated, with upwards of 30% of the mature channel structure comprised of extracellular carbohydrate. It is established that gating of many Na_v and voltage-gated K⁺ channel (K_v) isoforms can be altered directly by small changes in ion channel glycosylation (for additional details, please refer to [4]) [4–26].

Most studies established that sugar-dependent gating effects were imposed primarily by the terminal residue, sialic acid. An electrostatic mechanism was often assigned, with negatively charged sialic acids contributing to the surface potential, causing channels to gate following smaller depolarizations. Data also suggest that altered Na_v sialylation directly impacts cardiac and neuronal excitability [4,17,27–36].

Previously, the impact of sialic acids on gating of the human adult skeletal muscle voltage-gated Na_v channel, Na_v1.4 (hSkM1) was described, showing that sialic acids modulated all measured voltage-dependent gating parameters similarly [5,6]. That is, reductions in sialic acids shifted channel activation, inactivation, and recovery from inactivation toward depolarized potentials, likely through electrostatic mechanisms in which sialic acids contributed to a negative external surface potential. The D1S5–S6 extracellular loop of Na_v1.4 is heavily N-glycosylated, containing eight putative N-glycosylation sites, five of which are localized within a 24–30 amino acid repeat sequence that is unique to Na_v1.4. Interestingly, the deletion of this

heavily N-glycosylated D1S5–S6 repeat region was sufficient to eliminate only ~1/2 of the effects of sialic acids on $\text{Na}_v1.4$ gating as observed in the sialic acid deficient Lec2 CHO cell line, or following enzymatic desialylation using neuraminidase [6]. The additional effect of sialic acids on $\text{Na}_v1.4$ gating was explained at the time by a potential impact of the additional N-glycosylation sites within the $\text{Na}_v1.4$ primary sequence.

Later, all functionally relevant (to gating) sialic acid residues were shown to be localized to the $\text{Na}_v1.4$ D1S5–S6 extracellular loop using a set of $\text{Na}_v1.4$ and $\text{Na}_v1.5$ chimeras [5]. Specifically, sialic acids had no impact on gating of an $\text{Na}_v1.4$ chimera in which the D1S5–S6 loop of the major cardiac isoform $\text{Na}_v1.5$, which is typically not affected by sialic acids when expressed in CHO cells, replaced the analogous $\text{Na}_v1.4$ loop. Thus, as expressed in CHO cells, all functionally relevant sialic acids were shown to be localized to the $\text{Na}_v1.4$ D1S5–S6 loop. Mutagenic studies indicated that ~1/2 of the effect of sialic acids on $\text{Na}_v1.4$ gating is localized to the five N-glycan structures within the D1S5–S6 loop [6]. The source of the remaining effect of D1S5–S6 sialic acids on $\text{Na}_v1.4$ gating remains unknown.

Glycoproteins contain extracellular glycans attached to the protein through N- and O-linkages, with most previous efforts focusing on the role of N-glycans in VGIC gating. One reason for this is that there is a well-established consensus sequence required for N-glycosylation, but no such conserved sequence has been established as required for O-glycosylation, with the exception of an extracellular serine or threonine residue [37]. Thus, while determining putative N-glycosylation sites is obvious, it is not straightforward to determine potential O-glycosylation sites, particularly for VGIC with large extracellular loops that contain many serine and threonine residues.

Recently gating of three K_v isoforms, $\text{K}_v2.1$, $\text{K}_v4.2$, and $\text{K}_v4.3$, were shown to be modulated by sialic acids attached to O-glycans [13]. None of the three isoforms are N-glycosylated. When channel sialylation was reduced, gating of each K_v isoform was modulated through electrostatic mechanisms resulting in a depolarizing shift in channel activation voltage but with no effect on steady state inactivation.

It is clear from previous work that sialic acids attached to D1S5–S6 N-glycans contribute significantly to $\text{Na}_v1.4$ gating. O-glycans can also contribute to voltage-gated ion channel activity, at least to K_v channel activity [13,38]. Here we question whether sialic acids attached to $\text{Na}_v1.4$ O-glycans are responsible for the additional effect of D1S5–S6 sialic acids on $\text{Na}_v1.4$ gating. The D1S5–S6 linker of $\text{hNa}_v1.4$ contains 10 serine and 13 threonine residues, which could serve as potential attachment sites for O-linked sialic acids. Using two sets of CHO cell lines with varying abilities to sialylate and to N- and O-glycosylate proteins, we show for the first time that sialic acids attached to N- and O-glycans within the D1S5–S6 linker of $\text{Na}_v1.4$ modulate Na_v gating through electrostatic mechanisms. Future efforts that question the impact of glycans on ion channel activity should include studies to determine the functional role of sialic acids attached to both N- and O-glycans.

2. Materials and methods

2.1. $\text{Na}_v1.4$ constructs and CHO cell transfections

The two $\text{Na}_v1.4$ constructs used here, $\text{Na}_v1.4$ and $\text{Na}_v1.4/1.5\text{D1S5–6}$, were constructed as described previously as hSKM1 and hSKM1P1, respectively [5]. Briefly, the wild type $\text{hNa}_v1.4$ (hSKM1) construct and an $\text{Na}_v1.4$ chimera, $\text{Na}_v1.4/1.5\text{D1S5–6}$, in which the D1S5–S6 loop of $\text{hNa}_v1.5$ replaced the $\text{hNa}_v1.4$ loop, were inserted into the pCDNA3.1 vector (Invitrogen), and were expressed in two sets of Chinese Hamster Ovary (CHO) cell lines, the Pro5/Lec2/Lec1 cell lines, and the LdLD cell lines [39–41]. Both sets of cell lines are well established systems useful in questioning the impact of extracellular glycosylation on glycoprotein or cellular activity because the different cell lines express glycoproteins under variable levels of N- and O-glycosylation [5–15,17,18,39–41].

The LdLD cell line allows expression of Na_v under conditions of full or partial N- and/or O-linked glycosylation as illustrated in Fig. 1. The LdLD cell line is mutant in the 4-epimerase enzyme, responsible for the epimerization of glucose into galactose residues [39–41]. Galactose (Gal) is added to N- and O-linked structures just prior to addition of sialic acid. Cells can be grown in the absence or presence of galactose, thereby putatively producing Na_v with truncated (no galactose or sialic acids) or full N-glycosylation, respectively. Similarly, O-linked glycosylation can be controlled through incubation with N-acetylgalactosamine (GalNAc), with full N- and O-glycosylation achieved by incubating cells with saturating levels of GalNAc and Gal. Here, three different conditions were used: 1) Fully glycosylating/sialylating (both galactose sugars in medium), 2) Full N-, no O-glycosylation/sialylation (just Gal in medium), or 3) No sialic acids added to N- or O-glycans (neither galactose sugar added). Theoretically, the addition of GalNAc only could produce N-glycans with sialic acids attached directly to GalNAc residues. However, it was shown previously that CHO cell N-glycans do not contain GalNAc linked to N-glycan structures, and thus, adding only GalNAc is effectively the same as adding no sugars relative to the state of channel sialylation [42]. Nonetheless, this condition was studied, and consistent with previous reports indicating that CHO cells do not form N-acetylglucosamine (GlcNAc)/GalNAc linkages, all biophysical measurements made here for the GalNAc incubated hSKM1 (and $\text{Na}_v1.4/1.5\text{D1S5–6}$) were nearly identical to those observed for the channels expressed in the absence of galactose sugars. Therefore, the condition of adding only GalNAc is not included in the subsequent data.

LdLD cells were grown in Ham's F-12 medium (CellGro), fortified with 2 mM Glutamine, 100 U/ml penicillin, 100 mg/ml streptomycin and 10% Fetal Bovine Serum (FBS). Following transfection of LdLD cells, no FBS was added to the growth medium, only the relevant galactose residue(s), using 20 μM Gal and 400 μM GalNAc.

The Pro5 cell line represents the control, or fully glycosylating line [43]. The Lec2 cell line is deficient in the CMP-sialic acid transporter and produces glycoproteins with essentially no sialic acid attached to either N- or O-glycans, and serves as a model for congenital disorders of glycosylation (CDG) type IIc [42–44]. The Lec1 line is deficient in the transferase, N-acetylglucosaminyltransferase I (GlcNAc-T1), interrupting the production of complex N-glycans being added to glycoproteins, thereby producing fewer complex, but mannose-rich N-glycosylation structures [42,43]. Thus, comparison of the impact on Na_v gating as expressed in Lec2 versus Lec1 cells allows one to characterize the effect of reduced sialylation on both N- and O-glycans (Lec2 expression – no N- or O-linked sialic acids) versus sialic acids attached to N- or O-glycans only (Lec1 cells allow normal O-glycosylation, but produce truncated N-glycosylation, and therefore, no N-linked sialic acids), and then compared to the fully sialylated (in Pro5 cells).

For Pro5, Lec1, and Lec2 cell lines, the growing medium included alpha Minimum Essential Medium (αMEM) with (Pro5, Lec1) ribo- or deoxyribonucleosides (Lec2) (Invitrogen), and 100 U/ml penicillin and 100 mg/ml streptomycin and 10% FBS.

CHO cells were transiently transfected as described previously [5]. Briefly, cells were exposed to 1 ml Opti-MEM (Invitrogen) medium containing 8 μl lipofectamine (Invitrogen) and 1–2 μg DNA, consisting of about 12% EGFP vector (Clontech) and about 88% sodium channel expression vector. Following a 5–24 h incubation at 37 °C in a 5% CO_2 humidified incubator, the medium was exchanged for normal, non-selective cell growing medium, and transfectants were used for experiments 48 (for biochemical analysis) or 72 (for electrophysiological analysis) hours post-transfection.

2.2. Immunoblot analysis

Immunoblot analysis was performed on Pro5 whole cell lysates exactly as described previously [5], loading 10–30 μg protein/lane. Briefly, lysates were prepared, denatured, and then loaded into the lanes of a minigel cast from 4.5–5% acrylamide. Blots were incubated

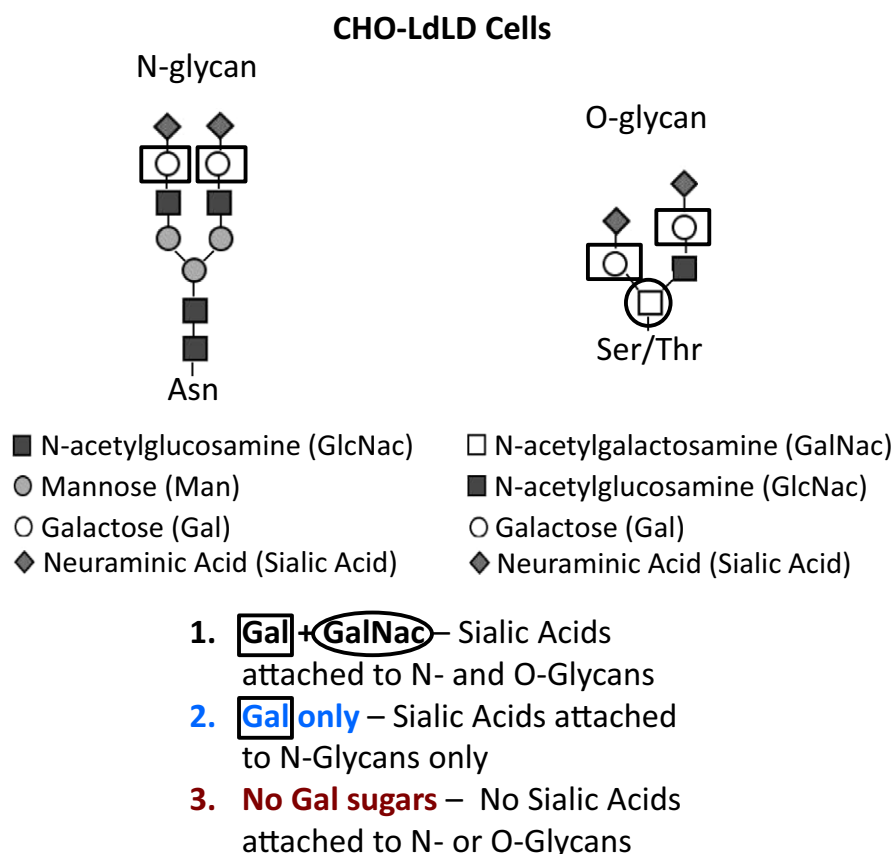


Fig. 1. Predicted N- and O-glycoprotein structures produced in LdLD cells when grown with and without galactose sugars. Left, predicted N-glycan structure. Right, predicted O-glycan structure. The residues that would not be added to the N- and O-glycans under each condition are boxed (Galactose) or encircled (GalNAc).

with a pan-specific anti- Na_v antibody overnight (1:200 dilution in 5% milk/HBS, as originally described in Bennett, 1999 [45]), followed by incubation with donkey anti-rabbit horse radish peroxidase secondary antibody (Amersham; 1:5000 dilution in 5% milk/HBS) for 2 h. Bands were visualized using a Pierce chemiluminescence kit. Because of the low levels of Na_v expression that results from the growth of cells without serum, it was not possible to perform biochemical studies on the transfected LdLD cells. Glycosidase treatments, which included sialidase A (to remove all sialic acids), N-glycanase (to remove N-linked glycan structures) and O-glycanase (to remove O-linked glycan structures) followed the manufacturer's published protocols (Glyko), incubating 1–2 μl glycosidase/sample for 1–3 h at 37 °C. Specifically, we incubated using the following units (U) glycosidase/sample: 0.01 U Sialidase A; 5.0 mU N-glycanase; 2.5 mU O-glycanase. Prior treatment with Sialidase A was necessary to remove terminal sialic acids in order for the O-glycanase to access and remove the underlying O-glycans. Relative apparent molecular weight (MW) was determined as previously described [34]. Briefly, scanned film was analyzed using ImageJ. The log of each MW marker was plotted versus its distance in arbitrary units traveled into the gel. A linear regression was then performed and used to calculate the MW of glycosidase-treated and untreated protein and to compare shifts in MW among treated and untreated conditions (in kilodaltons; kD).

2.3. Whole cell Na^+ current recordings

Transfected cells were studied using the patch-clamp whole-cell recording technique as previously described [5]. Experiments were done using an Axon Instruments 200B patch-clamp amplifier with a CV203BU headstage (Axon Instruments) used in combination with a

Nikon TE300 inverted microscope at room temperature (22 °C). The pulse protocols were generated using pulse acquisition software (HEKA). The resulting analog signals were filtered at 5 kHz and then digitized using the ITC-16 AD/DA converter (Instrutech). A micromanipulator (MP-285 Sutter, Novato, CA, USA) was used to place the electrode on the cell. Electrode glass (Drummond capillary tubes) was pulled using a Sutter (model P-87) electrode puller to resistances of 1–2 M Ω . All data were series resistance compensated to 95–98%. If proper compensation was not achieved, the data were not analyzed.

The external solution used was (mM): 224 Sucrose, 22.5 NaCl, 4 KCl, 2.0 CaCl_2 , 5 glucose, and 5 Hepes, while the internal solution used was (mM): 120 sucrose, 60 CsF, 32.5 NaCl, and 5 Hepes (titrated with 1 N NaOH to pH 7.4 at room temperature. Although series resistance was compensated 95–98% for all experiments, the smaller current produced using the low $[\text{Na}^+]$ solutions further minimized any remaining error due to series resistance to <1 mV, as described by us previously [46]. Current densities measured showed no systematic variation with respect to the glycosylation level of a specific isoform. Current amplitudes appeared to vary randomly as would be expected with transient transfections.

For experiments shown in Fig. 4 in which external Ca^{2+} levels were changed, seals were formed using the solutions described above. The lower external Ca^{2+} solution (0.2 mM) was then perfused at about 0.4 ml/min through a 100 mm pipette onto the cell starting at least 5 min following attainment of the whole cell configuration. At the start of perfusion, immediate measurements under 2.0 mM external Ca^{2+} were made — possible because of a small 'dead space' of approximately 0.6 mls in the perfusion apparatus filled with control solution. This protocol allowed measurements of control (2.0 mM Ca^{2+})

conditions during perfusion just prior to measurements made under lowered external Ca^{2+} conditions, removing any artifacts due to changes in pressure caused by the perfusion. The measured shifts in the voltages of half-activation (V_a) with changing external Ca^{2+} levels were reversible.

2.4. Pulse protocols

2.4.1. Conductance–voltage (G – V) relationship

Pulse protocols were performed as previously described [5] using a -120 mV holding potential. Lec1 cell line electrophysiology experiments were performed concurrently with the Pro5 and Lec2 cell lines studies that were previously reported [5]. The cells were stepped for 10 ms from the holding potential to various depolarized potentials, ranging from -100 mV to $+40$ mV in 10 mV increments. Consecutive pulses were stepped every 1.5 s and the data were leak subtracted using the P/4 method, stepping negatively from the holding potential. At each test potential, steady-state whole-cell conductance was determined by measuring the peak current at that potential and dividing by the driving force (i.e., difference between the membrane potential and the observed reversal potential). Peak conductance as a function of membrane potential was plotted. The maximum sodium conductance for a single cell was determined following single Boltzmann fits to the data (Eq. (1), solving for maximum conductance). The mean $V_a \pm \text{SEM}$ and $K_a \pm \text{SEM}$ values shown in Tables 1, 2 and listed in the legend to Fig. 5, were determined from these data fits. From the Boltzmann fits, the normalized data were then averaged with those from other cells, and the resultant average conductance–voltage curve was determined using the following Boltzmann relation fit to the data:

$$\text{Fraction of maximal conductance} = [1 + (\exp(-(V - V_a)/K_a))]^{-1} \quad (1)$$

where V is the membrane potential, V_a is the voltage of half activation, and K_a is the slope factor.

2.4.2. Steady-state inactivation (SSI) curves

Cells were first prepulsed for 500 ms from the holding potential to the plotted potentials ranging from -130 to -20 mV in 10 mV increments, then to a $+40$ mV test pulse for 5 ms. Currents from each cell were normalized to the maximum current measured by single Boltzmann fits to the data from a single cell (Eq. (2), solving for maximum current), from which the mean $V_i \pm \text{SEM}$ and $K_i \pm \text{SEM}$ values shown in Tables 1, 2 and listed in the legend to Fig. 5, were determined. As with steady state activation, the slope factors (K_i) were not significantly different among conditions.

From the Boltzmann fits, the normalized data for many cells were then averaged and the following Eq. (2) was fit to these data to produce the least squares fit curves:

$$\text{Fraction of maximum current} = [1 + (\exp(-(V - V_i)/K_i))]^{-1}, \quad (2)$$

where V is the membrane potential, V_i is the voltage of half inactivation, and K_i is the slope factor.

2.4.3. Measurement of inactivation time constants (τ_h)

Inactivation time constants were determined by fitting to single exponential functions the attenuating portions of the current traces used to measure the G – V relationships.

2.4.4. Recovery from inactivation

Cells were held at -120 mV, pulsed to $+40$ mV for 10 ms, and then stepped to the -100 mV recovery potential for 1 to 20 ms in 1 ms increments, with a 1.5 s delay between consecutive pulses. Following the recovery pulse, the potential was again stepped to $+40$ mV for 10 ms. The peak currents measured during the two $+40$ mV depolarizations were compared to determine the fractional current (recovery) measured during the second pulse. The fractional current was plotted as a function of the recovery time (in ms) between the two test pulses to $+40$ mV. Single exponential functions were fit to the data to determine the time constants for recovery from fast inactivation, τ_{rec} .

2.5. Statistical analysis

For data collected, the mean $\pm \text{SEM}$ were determined. ANOVA, tukey test, and Student's t -test were used where applicable and $p < 0.05$ was considered statistically significant.

3. Results

3.1. Galactose sugars added to LdLD cell medium resulted in altered $\text{Na}_v1.4$ gating with no impact on gating of the chimera, $\text{Nav1.4}/1.5\text{DIS5-6}$

To question whether sialic acids attached to N-glycans within the DIS5–S6 linker are responsible fully for the impact of sialic acids on $\text{Na}_v1.4$ gating, we expressed $\text{Na}_v1.4$ in LdLD cell lines in the presence and absence of galactose sugars to produce $\text{Na}_v1.4$ under three glycosylation/sialylation conditions as described in the Materials and methods section and illustrated in Fig. 1. All three sets of conditions produced voltage-gated Na^+ currents with similar characteristics and of

Table 1

The mean $\pm \text{SEM}$ gating parameter values measured for $\text{Na}_v1.4$ and $\text{Nav1.4}/1.5\text{DIS5-6}$ as expressed in LdLD cells. V_a , half activation voltage; K_a , Boltzmann slope factor for activation; V_i , half inactivation voltage; K_i , Boltzmann slope factor for inactivation; τ_{inact} , time constant for fast inactivation at -40 mV for $\text{Na}_v1.4$ and -30 mV for $\text{Nav1.4}/1.5\text{DIS5-6}$; τ_{rec} , time constant for recovery from fast inactivation at a -100 mV recovery potential. Significance ($p < 0.05$) tested comparing full glycosylation to each condition of reduced sialylation (*) and comparing between conditions of reduced sialylation (#).

Condition	n	V_a (mV)	K_a (mV)	V_i (mV)	K_i (mV)	τ_{inact} (ms)	τ_{rec} (ms)
$\text{Na}_v1.4$ (Full)	7	-31.2 ± 1.6	8.3 ± 0.4	-75.9 ± 2.0	-7.0 ± 0.6	2.2 ± 0.2	6.9 ± 0.6
$\text{Na}_v1.4$ (N-linked only)	10	$-24.8 \pm 2.8^{*,\#}$	9.4 ± 0.5	$-69.3 \pm 2.7^{*,\#}$	-7.8 ± 0.5	$3.6 \pm 0.5^{*,\#}$	$4.0 \pm 0.2^{*,\#}$
$\text{Na}_v1.4$ (No N- or O-linked)	13	$-14.1 \pm 1.5^{*,\#}$	9.7 ± 0.7	$-61.1 \pm 1.8^{*,\#}$	-7.3 ± 0.3	$6.4 \pm 0.8^{*,\#}$	$3.2 \pm 0.1^{*,\#}$
$\text{Nav1.4}/1.5\text{DIS5-6}$ (Full)	4	-20.2 ± 2.8	10.6 ± 0.7	-75.0 ± 3.7	-7.7 ± 0.7	3.0 ± 0.6	5.1 ± 0.6
$\text{Nav1.4}/1.5\text{DIS5-6}$ (N-linked only)	6	-19.9 ± 3.8	10.4 ± 0.9	-76.9 ± 1.6	-7.4 ± 0.4	3.0 ± 0.7	5.2 ± 0.5
$\text{Nav1.4}/1.5\text{DIS5-6}$ (No N- or O-linked)	7	-18.8 ± 2.2	10.5 ± 0.3	-77.1 ± 2.1	-7.6 ± 0.3	3.1 ± 0.4	5.1 ± 0.4

Table 2

The mean \pm SEM gating parameter values measured for $\text{Na}_v1.4$ and Nav1.4/1.5DIS5-6 as expressed in CHO cells. V_a , half activation voltage; K_a , Boltzmann slope factor for activation; V_i , half inactivation voltage; K_i , Boltzmann slope factor for inactivation; τ_{inact} , time constant for fast inactivation at -40 mV; τ_{rec} , time constant for recovery from fast inactivation at a -100 mV recovery potential. Significance ($p < 0.05$) tested comparing full glycosylation to each condition of reduced glycosylation (*) and comparing between conditions of reduced glycosylation (#). +Note, the data listed for Pro5 and Lec2 cells are italicized to reflect the fact that they were previously published (see Bennett, 2002 [5]).

Condition	n	V_a (mV)	K_a (mV)	V_i (mV)	K_i (mV)	τ_{inact} (ms)	τ_{rec} (ms)
<i>Pro5⁺</i>	9	-31.3 ± 2.0	7.4 ± 0.3	-71.5 ± 3.3	-5.9 ± 0.3	2.4 ± 0.4	3.62 ± 0.03
<i>Lec1</i>	4	$-22.8 \pm 2.4^{*,\#}$	8.9 ± 1.0	$-64.1 \pm 1.7^*$	$-6.9 \pm 0.4^*$	$3.5 \pm 0.3^{*,\#}$	$2.99 \pm 0.07^{*,\#}$
<i>Lec2⁺</i>	9	$-16.7 \pm 1.7^{*,\#}$	8.7 ± 0.6	$-60.8 \pm 1.5^*$	$-8.3 \pm 0.5^{*,\#}$	$7.9 \pm 1.1^{*,\#}$	$2.21 \pm 0.03^{*,\#}$

similar densities. Fig. 2A shows typical whole cell current traces from LdLD cells following incubation with both or no galactose sugars.

Steady-state voltage dependent channel gating was compared among glycosylation conditions to question whether variable glycosylation and sialylation achieved through incubation with different (or no) galactose sugars can lead to altered Na_v gating (Fig. 2, Table 1). The Na_v conductance–voltage (G–V) relationships were directly impacted by the varied conditions for glycosylation (Fig. 2B). Compared to fully glycosylating conditions (saturating levels of both galactose sugars), the G–V curve and voltage of half activation (V_a , see Table 1) were depolarized by ~ 17 mV in the absence of galactose sugars (no Na_v sialylation), and by ~ 7 mV in the presence of Gal only (this should allow full N-

glycosylation and sialylation but no O-glycosylation). There was no measurable impact of variable glycosylation on $\text{Na}_v1.4/1.5DIS5-6$ gating (Figs. 2D, E) indicating, as shown previously, that all functional $\text{Na}_v1.4$ sialic acids are localized to the D1S5–S6 linker. In addition, because both Na_v constructs were expressed under identical conditions in the same cell line with $\text{Na}_v1.4$ gating but not $\text{Na}_v1.4/1.5DIS5-6$ gating affected by variable glycosylation, the data also suggest that there is minimal to no effect of CHO cell sialolipids on Na_v gating. Together, these data suggest that sialic acids attached to D1S5–S6 N-glycans account for only $\sim 1/2$ of the effect of full D1S5–S6 sialylation on $\text{Na}_v1.4$ activation gating.

Previously, we showed that reduced channel sialylation modulates all voltage-dependent $\text{Na}_v1.4$ gating parameters similarly [5,6]. Thus,

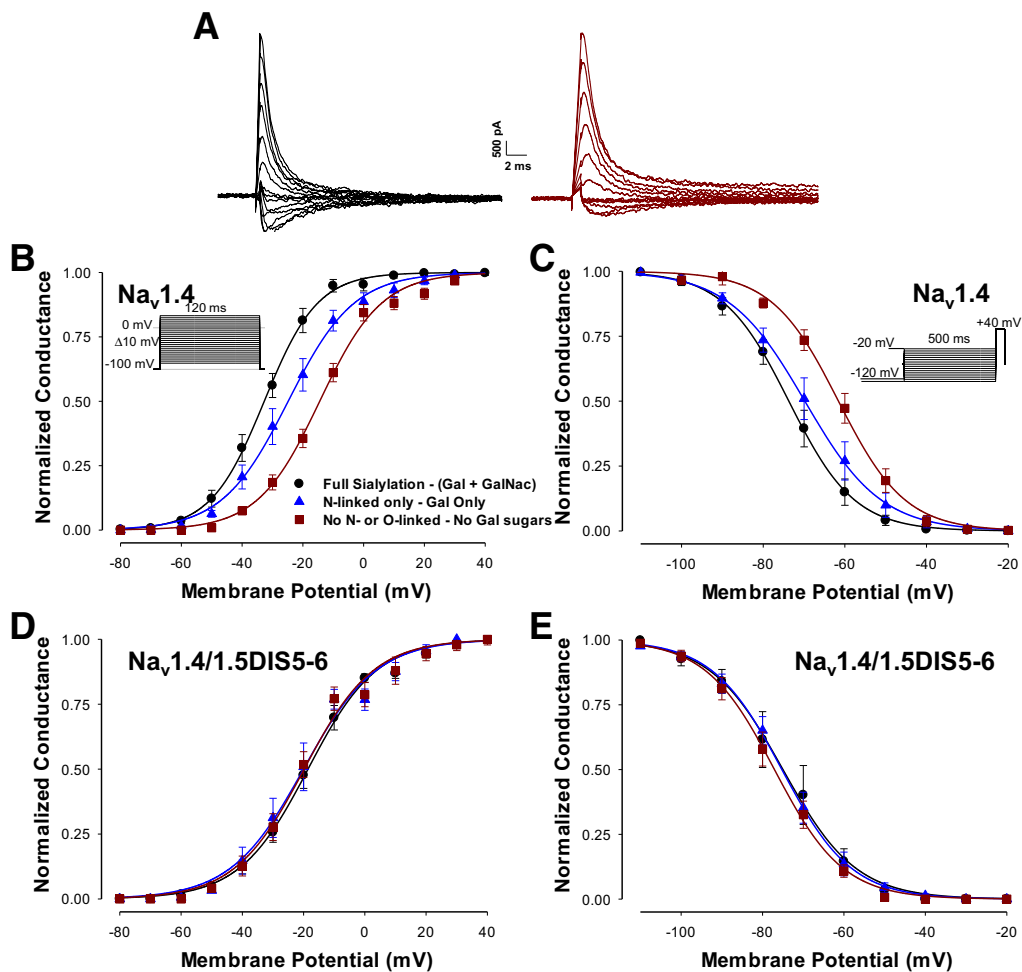


Fig. 2. Sialic acids attached to N-glycans account for only a portion of the effect of sialic acids on $\text{Na}_v1.4$ steady state gating. Here and throughout unless noted: 1) Full glycosylation (both Galactose sugars), black circles/lines; 2) Sialic acids attached to N-glycans only (Galactose only added), blue triangles/lines; 3) No sialylation (neither Galactose sugar), dark red squares/lines. A. Typical whole cell Na^+ current as measured under conditions of full (black, left) and no (dark red, right) sialylation. B. Steady-state activation (conductance–voltage, G–V) relationships for $\text{Na}_v1.4$. Inset, pulse protocol. C. Steady-state inactivation curves for $\text{Na}_v1.4$. Inset, pulse protocol. D. G–V curves for $\text{Na}_v1.4/1.5DIS5-6$. E. Steady-state inactivation curves for $\text{Na}_v1.4/1.5DIS5-6$. Data are the mean \pm SEM and are fit to single Boltzmann relationships (lines). Significance ($p < 0.05$) tested comparing full glycosylation to each condition of reduced sialylation (*) and comparing between conditions of reduced sialylation (#). n = 4–13 as listed in Table 1.

we measured and compared the voltage dependence of $\text{Na}_v1.4$ and $\text{Na}_v1.4/1.5\text{DIS5-6}$ steady-state inactivation (SSI) under the three glycosylation conditions (Fig. 2C, E). Note that the SSI and voltage of half-inactivation ($V_{1/2}$, see Table 1) for $\text{Na}_v1.4$ were also shifted toward depolarized potentials under conditions of no and N-only glycosylation compared to fully glycosylating/sialylating conditions (15 and 7 mV, respectively). There were no differences in the $\text{Na}_v1.4/1.5\text{DIS5-6}$ SSI curves among glycosylating conditions (Figs. 2E). These data indicate that the functional D1S5–S6 $\text{Na}_v1.4$ sialic acids impact SSI gating similarly to their effect on steady state channel activation, and that sialic acids linked to N-glycans account for only $\sim 1/2$ – $2/3$ of the effect of sialic acids on $\text{Na}_v1.4$ steady-state inactivation.

The rates at which $\text{Na}_v1.4$ and $\text{Na}_v1.4/1.5\text{DIS5-6}$ inactivate and recover from fast inactivation under the three conditions of glycosylation were also measured (Fig. 3). The data indicate that the kinetics of channel gating are similarly impacted by sialic acids, and that sialic acids linked to $\text{Na}_v1.4$ N-glycans account for $\sim 1/2$ – $2/3$ of the effect of sialic acids on channel kinetics. Similar to steady state gating, $\text{Na}_v1.4/1.5\text{DIS5-6}$ gating kinetics were unaffected by variable glycosylation. Table 1 lists the measured mean steady-state and kinetic gating parameters \pm SEM for $\text{Na}_v1.4$ and $\text{Na}_v1.4/1.5\text{DIS5-6}$ as expressed in LdLD cells under each glycosylation condition.

3.2. Sialic acids attached to N- and O-glycans modulate $\text{Na}_v1.4$ gating through apparent electrostatic mechanisms

To determine whether the dominant effect of variable sialylation on hSKM1 gating was conferred through electrostatic mechanisms,

$\text{Na}_v1.4$ G–V relationships in LdLD cells under different glycosylating conditions at two different external Ca^{2+} concentrations were determined (Fig. 4). Similar to our previous studies [5,6], the $\text{Na}_v1.4$ V_a under fully glycosylating conditions was most shifted at lower Ca^{2+} concentrations (~ 20 mV). There was only an ~ 7 mV shift in V_a observed under conditions of no sialylation, while the shift in V_a observed under conditions that allowed sialic acids to be attached to N-glycans was ~ 16 mV, intermediate between the shifts in V_a observed under fully and non-sialylated conditions. These data are completely consistent with our previous work and suggest that the functional sialic acids attached to the $\text{Na}_v1.4$ D1S5–S6 linker modulate channel gating through electrostatic mechanisms regardless of whether or not they are attached to N-glycans.

3.3. $\text{Na}_v1.4$ expressed under conditions that allow sialylation of O-glycans but not N-glycans also gate at voltages between those observed under conditions of full and no sialylation

The data generated using the LdLD cell line and incubating with variable types of galactose sugars clearly indicated that D1S5–S6 N-glycan sialic acids account for $\leq 2/3$ of the total impact of sialic acids on channel gating. It is possible that sialic acids attached to lipids that surround the channel protein could impact voltage-dependent channel gating [47]. However, as discussed previously, this is unlikely, as all experiments were performed on $\text{Na}_v1.4$ and $\text{Na}_v1.4/1.5\text{DIS5-6}$ under the same lipid environments, yet $\text{Na}_v1.4/1.5\text{DIS5-6}$ showed no sensitivity to changes in sialylation. These data indicate strongly that any contribution of sialolipids to Na_v gating in this system is immeasurable. Thus, we sought

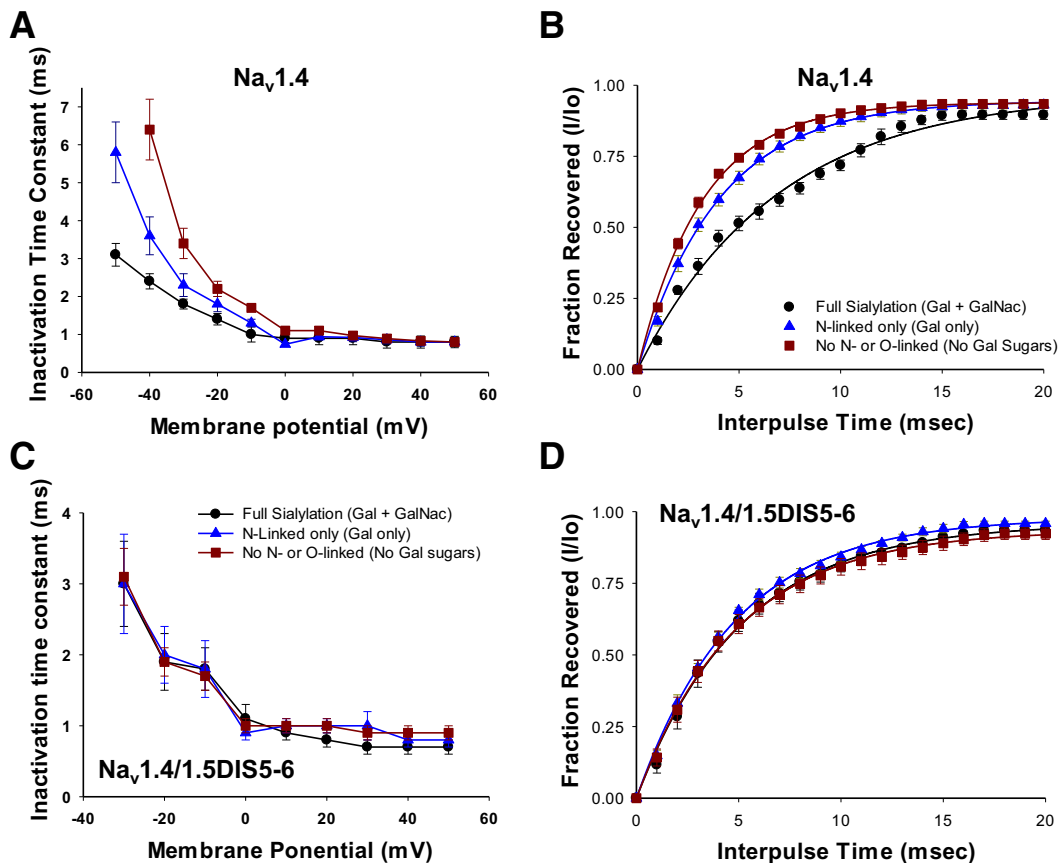


Fig. 3. Rates of fast inactivation and recovery from fast inactivation are modulated similarly under variable conditions of glycosylation. A. Time constants of fast inactivation as a function of test potential for $\text{Na}_v1.4$. B. $\text{Na}_v1.4$ fractional recovery from fast inactivation at a -100 mV recovery potential as a function of time. C. Fast inactivation time constants for $\text{Na}_v1.4/1.5\text{DIS5-6}$. D. Recovery time (at -100 mV) for $\text{Na}_v1.4/1.5\text{DIS5-6}$. Data are mean \pm SEM. Lines are non-theoretical, point-to-point. Significance ($p < 0.05$) tested comparing full glycosylation to each condition of reduced sialylation (*) and comparing between conditions of reduced sialylation (#).

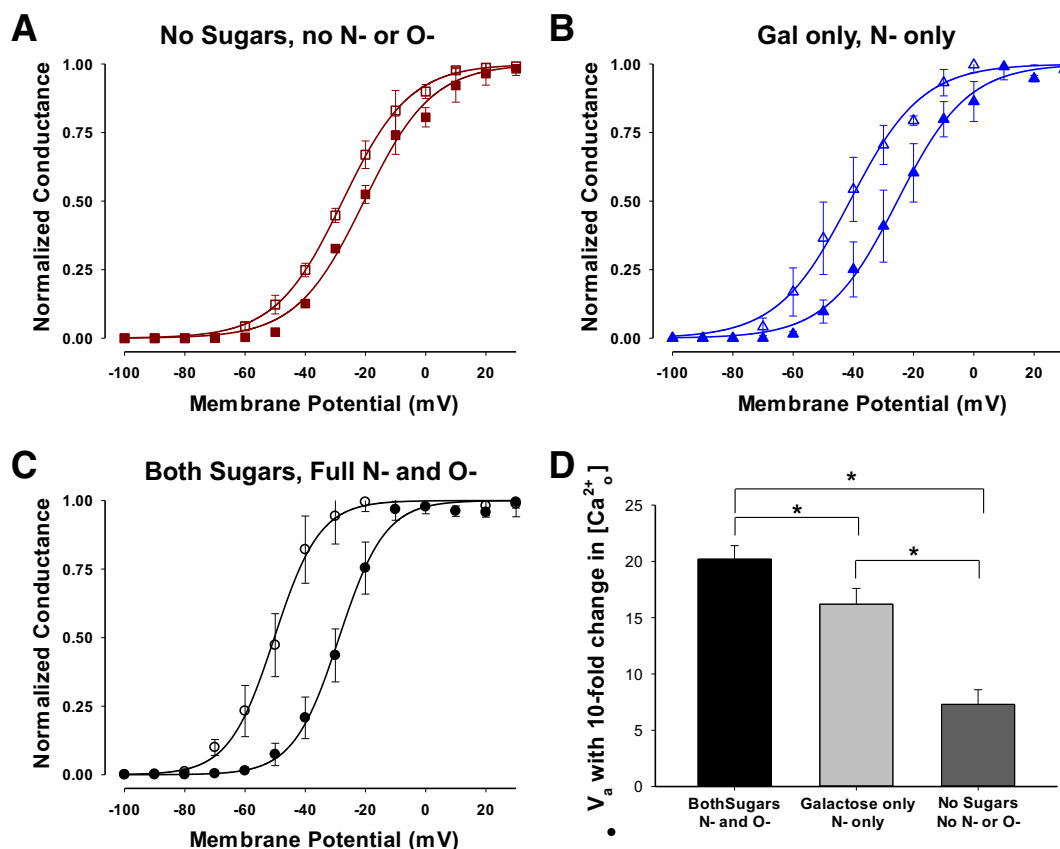


Fig. 4. Sialic acids modulate $\text{Na}_v1.4$ gating through electrostatic mechanisms. The V_a for $\text{Na}_v1.4$ expressed under conditions of full and two conditions of reduced sialylation were measured and compared at normal and low (10-fold reduction) external Ca^{2+} concentrations. A–C. G–V curves for $\text{Na}_v1.4$ under each glycosylation condition measured at 2.0 (solid symbols) and 0.2 (open symbols) mM Ca^{2+} . Data are the mean \pm SEM conductance at a membrane potential, and lines are fits of the data to single Boltzmann relationships. D. Data are mean hyperpolarizing shifts in V_a with a 10-fold reduction in external Ca^{2+} concentration (ΔV_a) \pm SEM. Note the significantly larger ΔV_a in the presence of sialic acids. Significance (*) tested comparing V_a shifts among conditions ($n = 3$; $p \leq 0.03$).

to question whether sialic acids attached to O-glycans also contribute to channel gating. For this, we expressed $\text{Na}_v1.4$ in the Lec1 CHO cell line, which, as described in the Methods section, is deficient in the transferase, N-acetylglucosaminyltransferase I (GlcNAc-T1), thereby interrupting the production of complex, but mannose-rich N-glycans [42,43]. By comparing $\text{Na}_v1.4$ gating in the Pro5 (fully glycosylating/sialylating parental CHO cell line), Lec2 (globally reduced sialylation, from both N- and O-glycans), and Lec1 (sialic acids attached only to O-glycans), we can question whether sialic acids attached to O-glycans contribute to $\text{Na}_v1.4$ gating, and if so, to what extent. Fig. 5A shows the predicted N- and O-glycan structures produced by each cell line as described in more detail in the Methods section. Expression of $\text{Na}_v1.4$ in Lec1 cells produced Na^+ currents with voltage-dependent steady state gating characteristics intermediate between those reported previously for $\text{Na}_v1.4$ expressed in the Pro5 and Lec2 cell lines (Figs. 5B, C) [5]. These data indicate that sialic acids attached to O-glycans are also responsible for modulating $\text{Na}_v1.4$ gating. Specifically, the V_a and V_i for $\text{Na}_v1.4$ expressed in Lec1 cells were 9 and 7 mV more depolarized than that observed for $\text{Na}_v1.4$ expressed in the fully sialylating Pro5 cells and were 6 and 3 mV more hyperpolarized than that observed for $\text{Na}_v1.4$ expressed in the non-sialylating Lec2 cells, respectively, with all measured voltage shifts being significant. The rates of fast inactivation and recovery from fast inactivation were affected similarly and consistently (See Table 2 for a summary of all mean \pm SEM gating parameters measured). Specifically, fast inactivation was significantly slower and recovery from fast inactivation was significantly faster in the less sialylated and less N-glycosylated CHO cells lines (Lec2 and Lec1, respectively) than that observed in the fully glycosylating Pro5 cell line. Further, the $\text{Na}_v1.4$ inactivation and recovery rates as expressed in Lec1 cells were

intermediate between the rates observed for $\text{Na}_v1.4$ expressed in Pro5 versus Lec2 cells and were significantly different from the Pro5 and Lec2 data. Together, the data strongly suggest that $\text{Na}_v1.4$ D1S5–S6 sialic acids attached to O-glycans contribute to voltage-dependent channel gating, accounting for $\sim 1/3$ – $1/2$ of the total effect of sialic acids on channel gating.

3.4. Sialic acids reside on N- and O-glycans attached to $\text{Na}_v1.4$

The biophysical data presented here indicate that $\text{Na}_v1.4$ is N- and O-glycosylated within the D1S5–S6 linker, and that sialic acids attached to N- and O-glycans modulate channel gating. To question more directly whether $\text{Na}_v1.4$ is N- and O-glycosylated and sialylated, we performed immunoblot gel shift analyses on Pro5 cells expressing $\text{Na}_v1.4$ (Fig. 6), similar to our previous efforts [35,36]. Here the gel shifts measured following sialidase and N-Glycanase treatments were similar to those reported by us previously for ventricular myocyte Na_v N-glycosylation [35,36]. A typical immunoblot is shown, with predicted apparent molecular weight (MW) calculated for each lane using Image J software listed at the bottom of each lane (see Methods for details). Table 3 lists the mean \pm SEM measured MW under each condition for 4–11 samples. The data indicate that $\text{Na}_v1.4$ D1S5–S6 contains N- and O-glycans that have sialic acids attached. Specifically, the mean, significant shift in MW for $\text{Na}_v1.4$ observed was 14 kD following sialidase treatment used to remove sialic acids, 37 kD following removal of sialic acids and O-glycans, 42 kD following removal of full N-glycans, and 51 kD following removal of sialic acids, O- and N-glycans. Together the data suggest that $\text{Na}_v1.4$ is N- and O-glycosylated, with both N- and O-glycans being sialylated.

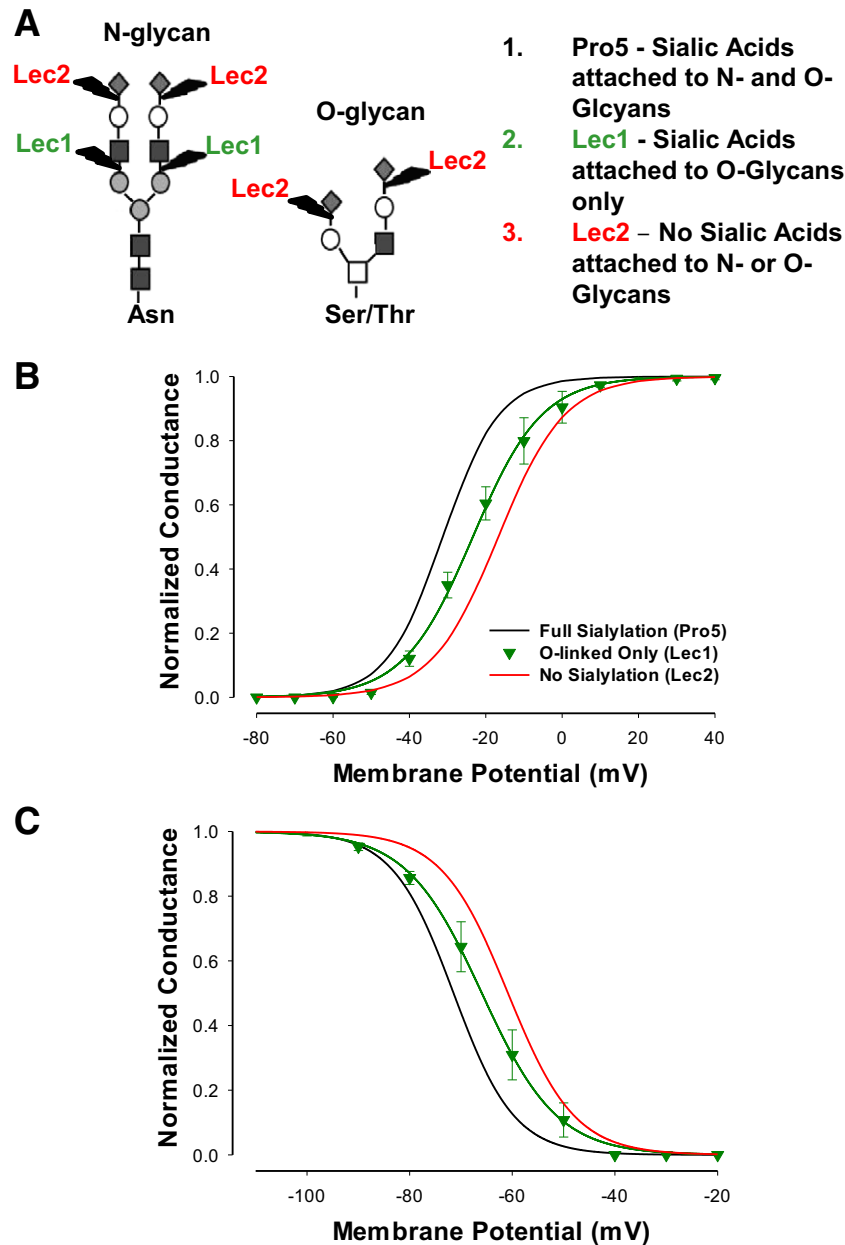


Fig. 5. Sialic acids attached to O-glycans modulate $\text{Na}_v1.4$ gating. **A.** Schematic of the expected glycan structures produced in Pro5, Lec1, and Lec2 cell lines as described in the Methods section. Sugar residue key as shown in Fig. 1 above. Lightning bolt indicates glycan linkages disrupted by the CHO cell line mutation. **B.** G–V relationships for $\text{Na}_v1.4$ expressed in Pro5 (full glycosylation, black line, $n = 9$), Lec1 (sialic acids attached to O-glycans only, green triangles/line, $n = 4$), and Lec2 (no sialic acids attached to N- or O- glycans, red line, $n = 9$). **C.** Steady-state inactivation for $\text{Na}_v1.4$ expressed in each cell line. Data are the mean \pm SEM and are fit to single Boltzmann relationships. Only Boltzmann curves are shown for the Pro5 and Lec2 data, as these data were presented in a previous report (see Bennett, 2002 [5]).

4. Discussion

4.1. Sialic acids attached to N- and O-glycans within the $\text{Na}_v1.4$ D1S5–S6 region modulate channel gating through electrostatic mechanisms

Here we demonstrate that the $\text{Na}_v1.4$ D1S5–S6 linker is N- and O-glycosylated and that the sialic acids attached to both N- and O-glycans modulate $\text{Na}_v1.4$ gating when expressed in two sets of CHO cell lines with varied abilities to glycosylate (and thereby sialylate) glycoproteins. The data clearly indicate that neither set of sialic acids (linked to N- or to O-glycans) can account fully for the impact of sialic acids on channel gating, but when attached to both N- and O-glycans, the full effect is realized (Figs. 2, 3, 5, 7). Further, sialic acids attached to N- and O-glycans within the $\text{Na}_v1.4$ D1S5–S6 linker modulate

$\text{Na}_v1.4$ gating through electrostatic mechanisms, with sialic acids attached to N- and O-glycans contributing approximately equally to channel gating.

4.2. Implications for future studies

The findings here have implications for future studies related to VGIC structure and function. That is, if N- and O-glycans can each contribute to VGIC gating and activity, then future studies investigating this phenomenon, should consider the impact of both N- and O-glycosylation. For example, we recently reported that sialic acids attached to the human ether-a-go-go (hERG) channel directly modulate hERG channel gating, effectively limiting hERG channel activity, resulting in a likely extension of the AP with increased sialylation [14].

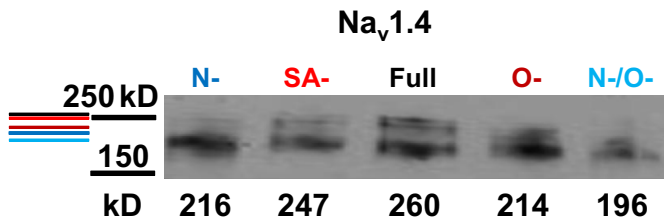


Fig. 6. Na_v1.4 is N- and O-glycosylated and sialylated. Representative immunoblot of Na_v1.4 as expressed in Pro5 cells with and without glycosidase treatments. Blot labels, lanes, (color): 1) N-, N-Glycanase treated to remove full N-glycan (blue); 2) SA-, Sialidase treated to remove all sialic acids (red); 3) Full, no glycosidase treatment, fully glycosylated (black); 4) O-, Sialidase and O-Glycanase treated to remove sialic acids and underlying O-glycan (dark red); and 5) N-/O-, Treatment using all three glycosidases (Sialidase, N-Glycanase, and O-Glycanase), to remove all Na_v sialic acids as well as N- and O-glycans (cyan). The mobility of the top band for each condition is shown to the left of the blot demarcated by a line of the same color as the lane label (from top to bottom: Full, SA-, O-, N-, and N-/O-). Apparent molecular weights of the top band are listed at the bottom of each lane.

No one prior to our recent study, questioned whether O-glycans attached to hERG also contribute to channel gating. We compared hERG channel gating as expressed in Pro5, Lec2, and Lec1 CHO cells lines, and showed that hERG channels gated similarly in the two sialic acid deficient cells lines (Lec2 and Lec1) compared to the fully sialylating cell line (Pro5). As described here, expression in the Lec2 cell line prevents sialylation of both N- and O-glycans, while expression in Lec1 cells allows sialic acids to attach to O-, but not N-glycans. Because hERG channels behaved similarly as expressed in both cell lines (unlike here), we can conclude that any sialic acids attached to hERG channel O-glycans do not contribute (measurably) to channel gating.

4.3. Na_v1.4 gating can be modulated by altering the level/types of substrates of N- and O-glycosylation

In addition to the novel finding that both N- and O-glycans contribute to Na_v1.4 gating, this is the first report to show that VGIC gating can be modulated by simply adding specific and different sugar residues to the culture medium of a mutant CHO cell line. Specifically, we showed in the LdLD cell line, that by adding galactose sugars to the culture medium, all measured voltage-dependent gating parameters for Na_v1.4 shifted to more hyperpolarized potentials compared to those measured under conditions with no galactose sugars added (Figs. 2, 3, 7 and Table 1). When N-acetylgalactosamine and galactose were added to the culture medium, Na_v1.4 SSA gating shifted to even more hyperpolarized potentials (by ~17 mV) compared to SSA gating in the absence of galactose sugars. These data suggest that simply by altering the availability of certain sugar substrates that are used in the glycosylation process, Na_v gating can be modulated, at least under conditions of genetically reduced glycosylation (for e.g., in individuals with Congenital Disorders of Glycosylation – see below). Apparently, because the voltage-dependent mechanisms of Na_v1.4 are finely tuned, very modest

changes in the amount/type of sugars that are attached to the channel can directly modulate channel gating and activity.

The Na_v window current, which is the region under the overlapping portions of the G–V and SSI curves, indicates the range of voltages and the extent to which Na_v are constitutively active. Any changes in Na_v window current would likely lead to altered channel activity that would modulate the overall electrical activity of a cell by impacting such parameters as threshold potential, action potential duration, etc. In Fig. 7, note how the voltage ranges of the peak window currents under conditions that allow sialic acids to be attached to either N- or O-glycans, are shifted to more depolarized potentials compared to the window current for Na_v functioning under fully glycosylating conditions. Further, under conditions of no channel sialylation, the window current is further shifted to the right, suggesting that sialic acids attached to each glycan type contribute to the window current and thereby to the constitutive activity of Na_v and the overall excitability of a cell.

4.4. Physiological and pathophysiological implications

We previously showed that developmentally regulated changes in Na_v glycosylation and specifically in Na_v sialylation, account fully for the differences in Na_v gating among cardiomyocyte types [36]. We went on to show that the cardiac glycome varies between atria and ventricles, and changes differentially during development of each cardiac chamber [35]. Our data also illustrated that the regulated expression of a single glycogene, the polysialyltransferase ST8Sia2, which in the mouse, is only expressed in the neonatal atria, was sufficient to modulate cardiomyocyte excitability [35]. That is, AP waveforms and gating of less sialylated Na_v were altered consistently in neonatal atrial myocytes but not in ventricular myocytes, when the ST8Sia2 gene was deleted.

There are a number of pathological states of reduced glycoprotein glycosylation, including a large family of congenital disorders of glycosylation (CDG) that contain approximately 40 different types resulting in multi-system effects and high infant mortality [48–62]. CDG, which are characterized by the glycogene that is mutated, cause variable but relatively modest reductions in glycoprotein N- or O-glycosylation, with reduced glycoprotein sialylation common to nearly all CDG. Those who suffer from CDG often present with severe cardiac and neuromuscular deficits, with the mechanisms responsible not fully understood. In a recent study, we began to question how the reduced sialylation that occurs in CDG patients might impact cardiac function. Thus, we showed that gene deletion of a single sialyltransferase that is uniformly expressed in the heart throughout development, ST3Gal4, was sufficient to reduce Na_v sialylation thereby resulting in modulated Na_v gating and reduced cardiomyocyte and epicardial refractory periods such that cardiomyocyte and ventricular conduction in the ST3Gal4^{−/−} animals were compromised, resulting in increased susceptibility to arrhythmias [34].

While this previous report focused on cardiac sialylation and its regulation as well as the pathophysiology associated with reduced, aberrant cardiac sialylation, there is little question that the skeletal muscle and neuronal glycomes are regulated as well [16]. Dietary and environmental factors such as alcohol abuse, obesity, smoking, and diabetes were also shown to contribute to altered glycosylation, suggesting that metabolic and/or environmental factors can contribute to glycosylation-induced pathologies [63]. With regulated and aberrant glycosylation, Na_v gating would likely be modulated, at least with respect to changes in channel sialylation. Thus, potential therapies could be developed exploiting the apparent susceptibility of Na_v to altered glycosylation such that any genetic and/or environmental factors that contribute to aberrant Na_v gating might be overcome, or at least attenuated, through therapies designed to alter Na_v glycosylation and thereby “return” Na_v gating back toward physiologic activity.

In our previous Na_v studies, we did not question whether sialic acid residues attached to N- versus O-glycans were both impacted and

Table 3

The mean ± SEM apparent molecular weights (MW) following glycosidase treatment(s) (in kD; n = 4–11). Significance (p < 0.05) was tested comparing MW measured with full glycosylation to the MW measured under each condition of reduced glycosylation (*), and the MW measured under non-sialylating conditions to the MW measured following removal of O- or N-glycans or both (#). The right column lists the average shift in MW measured following glycosidase treatment.

Condition	n	MW (kD)	ΔMW (kD from control)
Na _v 1.4			
Full Glycosylation	11	249 ± 1.9	N/A
Sialidase treated (SA-)	11	236 ± 2.5*	13
O-Glycanase treated (O-)	11	212 ± 2.5*,#	37
N-Glycanase treated (N-)	7	207 ± 3.7*,#	42
N- and O-Glycanase treated (N-/O-)	4	198 ± 1.9*,#	51

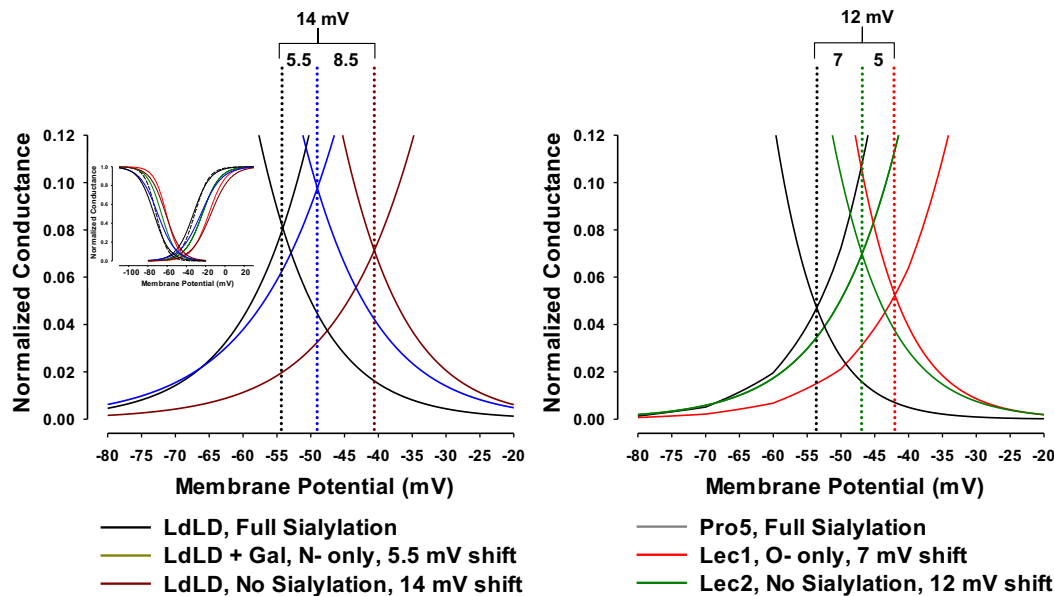


Fig. 7. $\text{Na}_v1.4$ window current is shifted to more depolarized potentials under conditions of reduced levels of sialic acids attached to N- and/or O-glycans. A: Larger scale of the overlapping steady-state activation (SSA) and inactivation (SSI) curves for $\text{Na}_v1.4$ as expressed in the LdLD cell line under each glycosylation condition tested. Inset: The full SSA and SSI curves for $\text{Na}_v1.4$ under all tested glycosylation conditions. B: Larger scale of the overlapping SSA and SSI curves for $\text{Na}_v1.4$ as expressed in the Pro5, Lec1, and Lec2 cell lines. Vertical lines indicate the membrane potential at which the peak window current occurs under each condition. The shift (in mV) in this peak window current voltage with altered glycosylation is listed on the top of the figure.

thereby altered Na_v gating [34–36]. Interestingly, the data shown here bolster the need to understand specifically the impact of N- versus O-glycosylation on Na_v gating, and how N- versus O-glycosylation changes physiologically and with disease. For example, because CDG typically affect either N- or O-glycosylation (both, in a few cases), the impact of CDG on Na_v gating and excitability would likely be dependent on the extent to which the CDG type limits sialylation of N- or O-glycans. Thus, our data here provide additional insight into a modulatory role for sialic acids attached to Na_v N- and O-glycans, and underscore the need of future studies to consider and characterize potential differential regulation and roles for sialic acid residues attached to N- versus O-glycans.

4.5. Summary and conclusions

Here we show for the first time that sialic acid residues attached to N- and O-glycans localized to the $\text{Na}_v1.4$ D1S5–S6 linker contribute to Na_v gating through electrostatic mechanisms. The relative contribution of sialic acids attached to N- versus O-glycans to the voltage dependence of $\text{Na}_v1.4$ gating was similar. Specifically, conditions that allow sialic acids to be attached to N- but not O-glycans or O- but not N-glycans, each produced intermediate shifts in voltage-dependent gating parameters compared to the shifts observed when sialylation was completely prevented. These data also indicated that there was no measurable impact of sialolipids on Na_v gating in this system. Immunoblot gel shift analyses support the biophysical data, suggesting that the $\text{Na}_v1.4$ D1S5–S6 linker has sialic acids attached to both N- and O-glycans. Together, the data indicate that sialic acids attached to the $\text{Na}_v1.4$ D1S5–S6 linker through N- and O-linkages contribute concurrently to channel gating through electrostatic mechanisms. Future studies should question the impact of both N- and O-glycans on VGIC gating and activity. In addition, as one questions how regulated and aberrant changes in cardiac, skeletal muscle, and neuronal glycosylation impact VGIC activity and overall excitability, relative changes in N- and O-protein glycosylation should be considered. Finally, these data suggest that Na_v gating can be modulated by exposure to altered levels of sugar residues that serve as substrates for N- and O-glycosylation, at least under certain conditions of reduced glycosylation. If intracellular sugar substrate

levels are altered in disease states such as diabetes, the glycosylation process would be affected, likely resulting in altered Na_v sialylation leading to modulated channel gating, AP waveforms and conduction.

Funding and acknowledgements

This work was supported, in part, by two research grants from the National Science Foundation, IOS-1146882 and CMMI-1266331, and a grant from the National Institutes of Health, NHLBI, 1R01HL102171.

References

- [1] A. Schroeter, S. Walzik, S. Blechschmidt, V. Haufe, K. Benndorf, T. Zimmer, Structure and function of splice variants of the cardiac voltage-gated sodium channel $\text{Na}_v1.5$, *J. Mol. Cell. Cardiol.* 49 (2010) 16–24.
- [2] C.A. Remme, C.R. Bezzina, Sodium channel (dys)function and cardiac arrhythmias, *Cardiovasc. Ther.* 28 (2010) 287–294.
- [3] G.S. Andavan, R. Lemmens-Gruber, Voltage-gated sodium channels: mutations, channelopathies and targets, *Curr. Med. Chem.* 18 (2011) 377–397.
- [4] A.R. Ednie, E.S. Bennett, Modulation of voltage-gated ion channels by sialylation, *Compr. Physiol.* 2 (2012) 1269–1301.
- [5] E.S. Bennett, Isoform-specific effects of sialic acid on voltage-dependent Na^+ channel gating: functional sialic acids are localized to the S5–S6 loop of domain I, *J. Physiol.* 538 (2002) 675–690.
- [6] E. Bennett, M.S. Urcan, S.S. Tinkle, A.G. Koszowski, S.R. Levinson, Contribution of sialic acid to the voltage dependence of sodium channel gating. A possible electrostatic mechanism, *J. Gen. Physiol.* 109 (1997) 327–343.
- [7] D. Johnson, E.S. Bennett, Gating of the shaker potassium channel is modulated differentially by N-glycosylation and sialic acids, *Pflügers Arch. - Eur. J. Physiol.* 456 (2008) 393–405.
- [8] D. Johnson, M.L. Montpetit, P.J. Stocker, E.S. Bennett, The sialic acid component of the $\beta 1$ subunit modulates voltage-gated sodium channel function, *J. Biol. Chem.* 279 (2004) 44303–44310.
- [9] W.B. Thornhill, I. Watanabe, J.J. Sutachan, M.B. Wu, X. Wu, J. Zhu, E. Recio-Pinto, Molecular cloning and expression of a $\text{Kv}1.1$ -like potassium channel from the electric organ of *Electrophorus electricus*, *J. Membr. Biol.* 196 (2003) 1–8.
- [10] W.B. Thornhill, M.B. Wu, X. Jiang, X. Wu, P.T. Morgan, J.F. Margiotta, Expression of $\text{Kv}1.1$ delayed rectifier potassium channels in Lec mutant Chinese hamster ovary cell lines reveals a role for sialidation in channel function, *J. Biol. Chem.* 271 (1996) 19093–19098.
- [11] I. Watanabe, J. Zhu, J.J. Sutachan, A. Gottschalk, E. Recio-Pinto, W.B. Thornhill, The glycosylation state of $\text{Kv}1.2$ potassium channels affects trafficking, gating, and simulated action potentials, *Brain Res.* 1144 (2007) 1–18.
- [12] T.A. Schwetz, S.A. Norring, E.S. Bennett, N-glycans modulate $\text{K}(v)1.5$ gating but have no effect on $\text{K}(v)1.4$ gating, *Biochim. Biophys. Acta* 1798 (2010) 367–375.

- [13] T.A. Schwetz, S.A. Norring, A.R. Ednie, E.S. Bennett, Sialic acids attached to O-glycans modulate voltage-gated potassium channel gating, *J. Biol. Chem.* 286 (2011) 4123–4132.
- [14] S.A. Norring, A.R. Ednie, T.A. Schwetz, D. Du, H. Yang, E.S. Bennett, Channel sialic acids limit hERG channel activity during the ventricular action potential, *FASEB J.* 27 (2013) 622–631.
- [15] D. Johnson, E.S. Bennett, Isoform-specific effects of the beta2 subunit on voltage-gated sodium channel gating, *J. Biol. Chem.* 281 (2006) 25875–25881.
- [16] L. Tyrrell, M. Renganathan, S.D. Dib-Hajji, S.G. Waxman, Glycosylation alters steady-state inactivation of sodium channel Nav1.9/NaN in dorsal root ganglion neurons and is developmentally regulated, *J. Neurosci. Off. J. Soc. Neurosci.* 21 (2001) 9629–9637.
- [17] C.A. Ufret-Vincenty, D.J. Baro, W.J. Lederer, H.A. Rockman, L.E. Quinones, L.F. Santana, Role of sodium channel deglycosylation in the genesis of cardiac arrhythmias in heart failure, *J. Biol. Chem.* 276 (2001) 28197–28203.
- [18] C.A. Ufret-Vincenty, D.J. Baro, L.F. Santana, Differential contribution of sialic acid to the function of repolarizing K(+) currents in ventricular myocytes, *Am. J. Physiol. Cell Physiol.* 281 (2001) C464–C474.
- [19] M.K. Hall, T.A. Cartwright, C.M. Fleming, R.A. Schwalbe, Importance of glycosylation on function of a potassium channel in neuroblastoma cells, *PLoS One* 6 (2011) e19317.
- [20] M.K. Hall, W. Reutter, T. Lindhorst, R.A. Schwalbe, Biochemical engineering of the N-acyl side chain of sialic acids alters the kinetics of a glycosylated potassium channel Kv3.1, *FEBS Lett.* 585 (2011) 3322–3327.
- [21] A. Pabon, K.W. Chan, J.L. Sui, X. Wu, D.E. Logothetis, W.B. Thornhill, Glycosylation of GIRK1 at Asn119 and ROMK1 at Asn117 has different consequences in potassium channel function, *J. Biol. Chem.* 275 (2000) 30677–30682.
- [22] Y. Zhang, H.A. Hartmann, J. Satin, Glycosylation influences voltage-dependent gating of cardiac and skeletal muscle sodium channels, *J. Membr. Biol.* 171 (1999) 195–207.
- [23] R.A. Schwalbe, L. Bianchi, A.M. Brown, Mapping the kidney potassium channel ROMK1. Glycosylation of the pore signature sequence and the COOH terminus, *J. Biol. Chem.* 272 (1997) 25217–25223.
- [24] R.A. Schwalbe, Z. Wang, L. Bianchi, A.M. Brown, Novel sites of N-glycosylation in ROMK1 reveal the putative pore-forming segment H5 as extracellular, *J. Biol. Chem.* 271 (1996) 24201–24206.
- [25] R.A. Schwalbe, Z. Wang, B.A. Wible, A.M. Brown, Potassium channel structure and function as reported by a single glycosylation sequon, *J. Biol. Chem.* 270 (1995) 15336–15340.
- [26] L.C. Freeman, J.J. Lippold, K.E. Mitchell, Glycosylation influences gating and pH sensitivity of I(sK), *J. Membr. Biol.* 177 (2000) 65–79.
- [27] D. Isaev, E. Isaeva, T. Shatskih, Q. Zhao, N.C. Smits, N.W. Shworak, R. Khazipov, G.L. Holmes, Role of extracellular sialic acid in regulation of neuronal and network excitability in the rat hippocampus, *J. Neurosci. Off. J. Soc. Neurosci.* 27 (2007) 11587–11594.
- [28] D. Isaev, Q. Zhao, J.K. Kleen, P.P. Lenck-Santini, D. Adstamongkonkul, E. Isaeva, G.L. Holmes, Neuroaminidase reduces interictal spikes in a rat temporal lobe epilepsy model, *Epilepsia* 52 (2011) e12–e15.
- [29] E. Isaeva, I. Lushnikova, A. Savrasova, G. Skibo, G.L. Holmes, D. Isaev, Blockade of endogenous neuraminidase leads to an increase of neuronal excitability and activity-dependent synaptogenesis in the rat hippocampus, *Eur J Neurosci.* 32 (2010) 1889–1896.
- [30] R. Islam, M. Nakamura, H. Scott, E. Repnikova, M. Carnahan, D. Pandey, C. Caster, S. Khan, T. Zimmermann, M.J. Zoran, V.M. Panin, The role of Drosophila cytidine monophosphate-sialic acid synthetase in the nervous system, *J. Neurosci. Off. J. Soc. Neurosci.* 33 (2013) 12306–12315.
- [31] E. Repnikova, K. Koles, M. Nakamura, J. Pitts, H. Li, A. Ambavane, M.J. Zoran, V.M. Panin, Sialyltransferase regulates nervous system function in Drosophila, *J. Neurosci. Off. J. Soc. Neurosci.* 30 (2010) 6466–6476.
- [32] H. Scott, V.M. Panin, The role of protein N-glycosylation in neural transmission, *Glycobiology* 24 (2014) 407–417.
- [33] H. Scott, V.M. Panin, N-glycosylation in regulation of the nervous system, *Adv. Neurobiol.* 9 (2014) 367–394.
- [34] A.R. Ednie, K.K. Horton, J. Wu, E.S. Bennett, Expression of the sialyltransferase, ST3Gal4, impacts cardiac voltage-gated sodium channel activity, refractory period and ventricular conduction, *J. Mol. Cell. Cardiol.* 59 (2013) 117–127.
- [35] M.L. Montpetit, P.J. Stocker, T.A. Schwetz, J.M. Harper, S.A. Norring, L. Schaffer, S.J. North, J. Jang-Lee, T. Gilmartin, S.R. Head, S.M. Haslam, A. Dell, J.D. Marth, E.S. Bennett, Regulated and aberrant glycosylation modulate cardiac electrical signaling, *Proc. Natl. Acad. Sci. U. S. A.* 106 (2009) 16517–16522.
- [36] P.J. Stocker, E.S. Bennett, Differential sialylation modulates voltage-gated Na⁺ channel gating throughout the developing myocardium, *J. Gen. Physiol.* 127 (2006) 253–265.
- [37] R.G. Spiro, Protein glycosylation: nature, distribution, enzymatic formation, and disease implications of glycopeptide bonds, *Glycobiology* 12 (2002) 43R–56R.
- [38] K.D. Chandrasekhar, A. Lvov, C. Terrenoire, G.Y. Gao, R.S. Kass, W.R. Kobertz, O-glycosylation of the cardiac I(Ks) complex, *J. Physiol.* 589 (2011) 3721–3730.
- [39] D.M. Kingsley, K.F. Kozarsky, L. Hobbie, M. Krieger, Reversible defects in O-linked glycosylation and LDL receptor expression in a UDP-Gal/UDP-GalNAc 4-epimerase deficient mutant, *Cell* 44 (1986) 749–759.
- [40] D.M. Kingsley, K.F. Kozarsky, M. Segal, M. Krieger, Three types of low density lipoprotein receptor-deficient mutant have pleiotropic defects in the synthesis of N-linked, O-linked, and lipid-linked carbohydrate chains, *J. Cell Biol.* 102 (1986) 1576–1585.
- [41] K. Kozarsky, D. Kingsley, M. Krieger, Use of a mutant cell line to study the kinetics and function of O-linked glycosylation of low density lipoprotein receptors, *Proc. Natl. Acad. Sci. U. S. A.* 85 (1988) 4335–4339.
- [42] S.J. North, H.H. Huang, S. Sundaram, J. Jang-Lee, A.T. Etienne, A. Trollope, S. Chalabi, A. Dell, P. Stanley, S.M. Haslam, Glycomics profiling of Chinese hamster ovary cell glycosylation mutants reveals N-glycans of a novel size and complexity, *J. Biol. Chem.* 285 (2010) 5759–5775.
- [43] P. Stanley, V. Caillibot, L. Siminovich, Selection and characterization of eight phenotypically distinct lines of lectin-resistant Chinese hamster ovary cell, *Cell* 6 (1975) 121–128.
- [44] I. Martinez-Duncker, T. Dupre, V. Piller, F. Piller, J.J. Candelier, C. Trichet, G. Tchernia, R. Oriol, R. Mollicone, Genetic complementation reveals a novel human congenital disorder of glycosylation of type II, due to inactivation of the Golgi CMP-sialic acid transporter, *Blood* 105 (2005) 2671–2676.
- [45] E.S. Bennett, Effects of channel cytoplasmic regions on the activation mechanisms of cardiac versus skeletal muscle Na⁺ channels, *Biophys. J.* 77 (1999) 2999–3009.
- [46] E.S. Bennett, Channel cytoplasmic loops alter voltage-dependent sodium channel activation in an isoform-specific manner, *J. Physiol.* 535 (2001) 371–381.
- [47] S. Cukierman, W.C. Zinkand, R.J. French, B.K. Krueger, Effects of membrane surface charge and calcium on the gating of rat brain sodium channels in planar bilayers, *J. Gen. Physiol.* 92 (1988) 431–447.
- [48] A. Almeida, M. Layton, A. Karadimitris, Inherited glycosylphosphatidyl inositol deficiency: a treatable CDG, *Biochim. Biophys. Acta* 1792 (2009) 874–880.
- [49] E.J. Footitt, A. Karimova, M. Burch, T. Yayeh, T. Dupre, S. Vuillaumier-Barrot, I. Chantret, S.E. Moore, N. Seta, S. Grunewald, Cardiomyopathy in the congenital disorders of glycosylation (CDG): a case of late presentation and literature review, *J. Inher. Metab. Dis.* 32 (Suppl.1) (2009) S313–S319.
- [50] H.H. Freeze, Towards a therapy for phosphomannomutase 2 deficiency, the defect in CDG-Ia patients, *Biochim. Biophys. Acta* 1792 (2009) 835–840.
- [51] S. Grunewald, The clinical spectrum of phosphomannomutase 2 deficiency (CDG-Ia), *Biochim. Biophys. Acta* 1792 (2009) 827–834.
- [52] J. Jaeken, Congenital disorders of glycosylation (CDG): it's (nearly) all in it! *J. Inher. Metab. Dis.* 34 (2011) 853–858.
- [53] J. Jaeken, Congenital disorders of glycosylation, *Ann. N. Y. Acad. Sci.* 1214 (2010) 190–198.
- [54] T. Marquardt, J. Denecke, Congenital disorders of glycosylation: review of their molecular bases, clinical presentations and specific therapies, *Eur. J. Pediatr.* 162 (2003) 359–379.
- [55] A.G. Woods, C.W. Woods, T.M. Snow, Congenital disorders of glycosylation, *Adv. Neonatal Care* 12 (2012) 90–95.
- [56] H.H. Freeze, E.A. Eklund, B.G. Ng, M.C. Patterson, Neurology of inherited glycosylation disorders, *Lancet Neurol.* 11 (2012) 453–466.
- [57] H.H. Freeze, Genetic defects in the human glycome, *Nat. Rev. Genet.* 7 (2006) 537–551.
- [58] H.H. Freeze, M. Aebi, Altered glycan structures: the molecular basis of congenital disorders of glycosylation, *Curr. Opin. Struct. Biol.* 15 (2005) 490–498.
- [59] K. Ohtsubo, J.D. Marth, Glycosylation in cellular mechanisms of health and disease, *Cell* 126 (2006) 855–867.
- [60] J.G. Leroy, Congenital disorders of N-glycosylation including diseases associated with O- as well as N-glycosylation defects, *Pediatr. Res.* 60 (2006) 643–656.
- [61] C. Kranz, A.A. Basinger, M. Gucavas-Calikoglu, L. Sun, C.M. Powell, F.W. Henderson, A.S. Aylsworth, H.H. Freeze, Expanding spectrum of congenital disorder of glycosylation Ig (CDG-Ig): sibs with a unique skeletal dysplasia, hypogammaglobulinemia, cardiomyopathy, genital malformations, and early lethality, *Am. J. Med. Genet. A* 143A (2007) 1371–1378.
- [62] M. Al-Owain, S. Mohamed, N. Kaya, A. Zagal, G. Matthijs, J. Jaeken, A novel mutation and first report of dilated cardiomyopathy in ALG6-CDG (CDG-Ic): a case report, *Orphanet J. Rare Dis.* 5 (2010) 7.
- [63] A. Knezevic, O. Polasek, O. Gornik, I. Rudan, H. Campbell, C. Hayward, A. Wright, I. Kolcic, N. O'Donoghue, J. Bones, P.M. Rudd, G. Lauc, Variability, heritability and environmental determinants of human plasma N-glycome, *J. Proteome Res.* 8 (2009) 694–701.